Electron tomography of the microtubule cytoskeleton in multinucleated hyphae of *Ashbya gossypii*

Romain Gibeaux[1], Claudia Lang[2], Antonio Z. Politi[1], Sue L. Jaspersen[3,4], Peter Philippsen[2,*,‡] and Claude Antony[1,‡]

[1]European Molecular Biology Laboratory (EMBL), Meyerhofstrasse 1, 69117 Heidelberg, Germany
[2]Molecular Microbiology, Biozentrum, University of Basel, Klingelbergstrasse 50-70, CH-4056 Basel, Switzerland
[3]Stowers Institute for Medical Research, 1000 E. 50th Street, Kansas City, MO 64110, USA
[4]Department of Molecular and Integrative Physiology, University of Kansas Medical Center, 3901 Rainbow Boulevard, Kansas City, KS 66160, USA

*Author for correspondence (peter.philippsen@unibas.ch)
‡These authors contributed equally to this work

Accepted 10 September 2012
Journal of Cell Science 125, 5830–5839

doi: 10.1242/jcs.111005

Summary

We report the mechanistic basis guiding the migration pattern of multiple nuclei in hyphae of *Ashbya gossypii*. Using electron tomography, we reconstructed the cytoplasmic microtubule (cMT) cytoskeleton in three tip regions with a total of 13 nuclei and also the spindle microtubules of four mitotic nuclei. Each spindle pole body (SPB) nucleates three cMTs and most cMTs above a certain length grow according to their plus-end structure. Long cMTs closely align for several microns along the cortex, presumably marking regions where dynein generates pulling forces on nuclei. Close proximity between cMTs emanating from adjacent nuclei was not observed. The majority of nuclei carry duplicated side-by-side SPBs, which together emanate an average of six cMTs, in most cases in opposite orientation with respect to the hyphal growth axis. Such cMT arrays explain why many nuclei undergo short-range back and forth movements. Only occasionally do all six cMTs orient in one direction, a precondition for long-range nuclear bypassing. Following mitosis, daughter nuclei carry a single SPB with three cMTs. The increased probability that all three cMTs orient in one direction explains the high rate of nuclear bypassing observed in these nuclei. The *A. gossypii* mitotic spindle was found to be structurally similar to that of *Saccharomyces cerevisiae* in terms of nuclear microtubule (nMT) number, length distribution and three-dimensional organization even though the two organisms differ significantly in chromosome number. Our results suggest that two nMTs attach to each kinetochore in *A. gossypii* and not only one nMT like in *S. cerevisiae*.

Key words: Filamentous fungus, Nuclear migration, Microtubule ends, Spindle pole body, Mitotic spindle

Introduction

In eukaryotic cells the dynamics of nuclei is closely associated with the microtubule cytoskeleton. Cytoplasmic microtubules (cMTs) are indispensible for migration and positioning of nuclei within the cell, and spindle microtubules (also known as nuclear microtubules, nMTs) are essential for positioning and segregation of chromosomes during nuclear division. In multinucleated filamentous fungi the cMT cytoskeleton has evolved into a complex system with the remarkable ability to control the migration and distribution of multiple nuclei in the same cell. The biological advantage of multinuclearity and nuclear dynamics in fungi is well known (Roper et al., 2011). However, the underlying mechanism to control the movements of multiple nuclei in fungal hyphae is not well understood.

Components of this control system were first identified in *Aspergillus nidulans* and *Neurospora crassa* by analyzing mutants exhibiting nuclear distribution defects. Several of the identified genes encoded subunits of the microtubule motor dynein and its activator dynactin (Minke et al., 1999; Morris, 2000; Xiang et al., 1994; Xiang and Fischer, 2004) strongly indicating that cMTs are part of the control system (Han et al., 2001; Minke et al., 1999; Zhang et al., 2003). Studies aiming at analyzing the contribution of cMTs in controlling nuclear migration were hampered by the fact that cMTs, in these and other filamentous fungi, are also important for organelle and vesicle transport (Schuster et al., 2011; Seiler et al., 1999; Wedlich-Söldner et al., 2002; Zekert and Fischer, 2009). A notable exception is *Ashbya gossypii* because, like in budding yeast, in this filamentous fungus cMTs are only involved in nuclear migration control and not in transport of other organelles or vesicles (Gladfelter et al., 2006; Köhli et al., 2008). Thus, mutations changing the structure or dynamics of cMTs in *A. gossypii* only affect nuclear migration and not other cellular processes, making it an ideal model system to study the cMT organization that supports multinuclearity.

Nuclei in *A. gossypii* hyphae show a complex cMT- and dynein-dependent migration pattern. All nuclei frequently perform autonomous short-range forward and backward movements with respect to the growth direction and some nuclei move over long distances, thereby bypassing adjacent nuclei (Alberti-Segui et al., 2001; Gladfelter et al., 2006). After nocodazole-induced depolymerization of MTs, these oscillatory and bypassing movements can no longer be seen and nuclei only passively move with the stream of the cytoplasm (Alberti-Segui et al., 2001; Lang et al., 2010a). The minus ends of cMTs are attached to the outer plaque (OP) of the spindle pole body (SPB)

that is embedded in the nuclear envelope throughout the *A. gossypii* life cycle much as it is in budding yeast (Jaspersen and Winey, 2004; Lang et al., 2010a). Surprisingly though, only one motor, the multi-subunit dynein, is responsible for both types of nuclear movements in *A. gossypii*. Promoter truncations of *AgDYN1*, which reduce the levels of dynein heavy chain, cause decreased frequencies of oscillatory and bypassing movements (Grava et al., 2011). Because dynein accumulates at the plus end of cMTs, especially of long cMTs, and exerts pulling forces on nuclei when growing cMTs slide along the hyphal cortex (Grava and Philippsen, 2010), the organization of cMT arrays emanating from the SPB of each nucleus should be a key factor in determining the direction and most likely also the duration of cMT-dependent pulling of nuclei. A high-resolution analysis of cMT arrays at SPBs from several adjacent nuclei will help to understand nuclear mobility in *A. gossypii* hyphae but has yet to be reported.

Bidirectional nuclear movements continue during metaphase and anaphase, and mitotic nuclei also rotate until the anaphase spindle becomes longer than the hyphal diameter (Alberti-Segui et al., 2001; Grava et al., 2011). It is not known what, if any, role nuclear microtubules (nMTs) play in these continuous movements. In the closely related yeast *Saccharomyces cerevisiae* and most eukaryotes, nuclear positioning prior to elongation of the spindle in anaphase is essential so that chromosomes are equally partitioned into mother and daughter cell following cell division. Because of its multinucleate nature and the fact that many nuclei are present within each compartment, nuclear positioning is not an issue in *A. gossypii* (Finlayson et al., 2011). Many of the same motor proteins and microtubule binding proteins involved in nuclear positioning are also required for spindle assembly, making analysis of function more complex. However, in *A. gossypii*, these factors appear to primarily affect cMT function (Lang et al., 2010b; Grava and Philippsen, 2010; Alberti-Segui et al., 2001), raising the interesting question of how the *A. gossypii* mitotic spindle is organized. Reconstruction of mitotic spindles observed by thin section electron microscopy (EM) showed that the haploid *S. cerevisiae* spindle is composed of 16 kinetochore MTs, one for each of the 16 chromosomes, and 4 to 6 inter-polar MTs (Winey et al., 1995). Nuclei of *A. gossypii* are haploid and carry only seven chromosomes (Dietrich et al., 2004). Like budding yeast, *A. gossypii* is thought to contain point centromeres, although its centromeric DNA sequence is slightly longer (~180 bp compared to ~125 bp in *S. cerevisiae*) (Dietrich et al., 2004; Cottarel et al., 1989). How these differences in chromosome number, centromere length and nuclear behavior are accommodated in the *A. gossypii* spindle can only be revealed from high-resolution structural analysis of its mitotic apparatus.

In this paper we present high-resolution 3D models of the cMT cytoskeleton of hyphal tip regions and nMTs of mitotic spindles, obtained by electron tomography of *A. gossypii*. Our goals were: (1) to refine published results obtained with live-cell imaging and classical EM about the number, length and orientation of cMTs emanating at SPBs; (2) to determine the ratio of growing and shrinking cMTs by analyzing the structure of cMT plus ends; (3) to find an explanation for the observation that nuclear bypassing occurs primarily in daughter nuclei after mitosis; (4) to count the number of nMTs nucleated at mitotic SPBs; and (5) to identify potential kinetochore and inter-polar MTs in mitotic spindles.

Results

Cytoplasmic MT interaction with the cell cortex

Young mycelia of *A. gossypii* were cryo-immobilized, freeze-substituted, plastic-embedded and cut into serial 300 nm thick sections. Using large-scale electron tomography (ET) we reconstructed hyphal section volumes and tracked the plasma membrane, the nuclear envelopes and MTs through these sections in three full hyphal tip regions each carrying four to five nuclei. This allowed us to generate 3D models for thorough characterization of the cMT cytoskeleton (Fig. 1A-C). On first inspection of these data, it appears that long and short cMTs emanate from each nucleus in different directions and that several nuclei are not spherical due to differently shaped protrusions the origin of which is presently unknown.

The control of nuclear movements and distances may depend on interaction of cMTs emanating from adjacent nuclei, but we found no indication that cMTs align with each other. This confirms nuclear autonomy with respect to nuclear movements (Lang et al., 2010a) and nuclear cycles (Gladfelter et al., 2006). However, four of the very long cMTs seen in Fig. 1A–C align with the hyphal cortex in the regions delineated by thick arrows. The electronic slice of one of these regions (Fig. 1C) is magnified in Fig. 1D and reveals a uniform distance of ~12 nm, smaller than the diameter of microtubules, to the plasma membrane. This strongly indicates controlled lateral contacts between cMTs and the hyphal cortex, most likely involving dynein (Grava and Philippsen, 2010). Two of the very long cMTs, marked by thin arrows, end at the hyphal tip at a distance of 247 and 81 nm and lack lateral plasma membrane contacts. These distances and orientation to the tip cortex do not suggest that such end-on contact with the plasma membrane would promote nuclear migration (Fig. 1E). This conclusion is supported by the fact that a capture-shrinkage-like mechanism was not observed *in vivo* (Grava and Philippsen, 2010). Tip-associated cMTs might rather serve in the distance control between nuclei and the hyphal tips (Lang et al., 2010b).

Cytoplasmic MT nucleation at SPBs

In *A. gossypii*, like in *S. cerevisiae*, the SPB is embedded in the nuclear envelope and serves as the sole microtubule organization center. The well-documented laminar structure of *S. cerevisiae* SPBs is conserved in *A. gossypii* except for the slightly enlarged OP, which is the site for nucleation of cMTs (Jaspersen and Winey, 2004; Lang et al., 2010a). Live-cell imaging of GFP-labeled cMT arrays in *A. gossypii* has revealed up to six short and long cMTs emanating from nuclei in different directions. The long cMTs frequently grow past adjacent nuclei (Lang et al., 2010a). Therefore, models attempting to explain nuclear autonomous movements were based on SPBs each nucleating an independent array of five to six cMTs with different lengths and orientations and with alternating contacts with the hyphal cortex (Lang et al., 2010a; Lang et al., 2010b; Grava and Philippsen, 2010). These models could partially explain nuclear-autonomous short-range bidirectional movements but not nuclear bypassing. In particular, they do not explain the observation that nuclei that have just completed mitosis (so called daughter nuclei) are more likely to be pulled over long distances in one direction thereby bypassing one or more nuclei than nuclei at other stages (Alberti-Segui et al., 2001; Gladfelter et al., 2006; Lang et al., 2010a). We hoped to refine the present models by

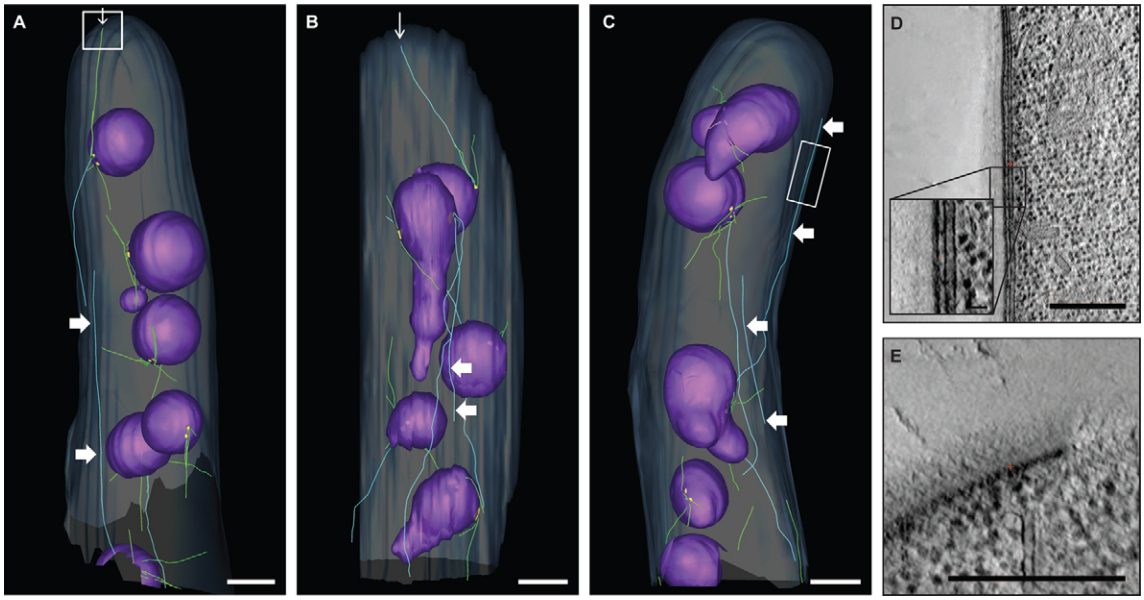

Fig. 1. cMT organization and interaction with the cell cortex. (**A–C**) Model views of cMT cytoskeleton arrays in three reconstructed hyphal tips containing a total of 14 nuclei. The plasma membrane is depicted in light blue, the nuclear envelope in purple, the SPBs in yellow, the short MTs in green and the long MTs in turquoise. Thin vertical arrows mark long cMTs pointing towards the hyphal tip, which is at the top for all three hyphae. Thick horizontal arrows delineate cMT segments following the plasma membrane with a regular spacing. These long cMTs interacting with the plasma membrane originate at the incompletely modeled sixth nucleus of hypha A, the mitotic nucleus at the tip of hyphae B, and at the third nucleus and a more distant nucleus in hypha C, as also seen from another orientation in Fig. 3. All cMTs are nucleated from an SPB. The cMTs that seem to lack a connection to an SPB have a connecting segment outside the area of acquisition that therefore could not be modeled. (**D**) Electron tomographic slice of the boxed area in C, showing a MT following the plasma membrane with a regular spacing of around 12 nm over a length of several microns. (**E**) Electron tomographic slice of the boxed area in A, showing a microtubule pointing towards the hypha tip. Scale bars: 1 μm (A–C); 300 nm (D,E).

tracing the nucleation sites of all cMTs visualized in the three hyphae in Fig. 1.

Snapshots of the origin of 14 cMT arrays are documented in Fig. 2. The shorter cMTs are colored in green, the long cMTs in blue, and the SPB central plaque (CP) is depicted in yellow. cMT minus ends are marked as red filled circles and the plus ends (seen in Fig. 2 for the very short cMTs) are shown in other colors to indicate different end structures (see below). Unexpectedly, cMTs at 12 of the 13 nuclei emanate from duplicated side-by-side not from single SPBs. The remaining nucleus, marked as B1, carries a metaphase spindle with two separate SPBs. Despite the limited number of investigated samples, the high percentage of side-by-side SPBs strongly indicates that the unduplicated SPB stage, most likely representing the G1 phase (Nair et al., 2010), is rather short compared to the duplicated SPB stage. Previously, it was already suggested that nuclei in *A. gossypii* can enter into S-phase very soon after mitosis (Gladfelter et al., 2006) implying a prolonged G2 phase with duplicated side-by-side SPBs. This is remarkably different from nuclear cycles of the evolutionary related yeast *S. cerevisiae*, which spend a relatively long period of time in G1 phase and have virtually no G2 phase (Lew and Reed, 1993). In fact it is very difficult to find side-by-side SPBs in *S. cerevisiae* cells by classical thin section electron microscopy (Byers and Goetsch, 1974; S.L.J., unpublished).

Another surprising result is the diversity of the cMT arrays emanating from side-by-side SPBs. Four types can be distinguished as summarized in Fig. 2D. Both SPBs nucleated cMTs in the same direction (Type 1: A4, B2) or each only in one but opposite directions (Type 2: B3, B5). Both SPBs nucleated cMTs in opposite directions (Type 3: A1, A3, C3, C4) or only one in opposite directions and another one in a single direction (Type 4: A2, B4, C1, C2). Ten of the twelve arrays, types 2 to 4, resemble the cMT arrays previously observed by *in vivo* fluorescence microscopy (Lang et al., 2010a) and could potentially pull nuclei alternatingly in both directions of the hyphal axis thereby generating short-range bidirectional movements. Irregular small angle rotations, observed for up to 50% of the nuclei (Lang et al., 2010a), could also be generated by such cMT arrays. Importantly, duplicated SPBs with type 1 arrays (Fig. 2A4, Fig. 2B2) could pull nuclei over long distances if one of the cMTs is very long and aligns with the cortex to induce pulling by the dynein complex (Grava and Philippsen, 2010). Therefore, the type 1 arrangement can fully explain the few cases of nuclei with duplicated side-by-side SPBs bypassing other nuclei.

It is not known whether the types of arrays shown in Fig. 2 are stable during a nuclear cycle or whether newly nucleated cMTs frequently modify the arrangement of cMTs. Assuming that most of the arrays shown in Fig. 2 are rather stable until the end of mitosis, 50% of the mitotic daughter nuclei should be attached to cMTs pointing into one direction and thus could be pulled long distances explaining the observed high frequency of bypassing events directly after mitosis (Alberti-Segui et al., 2001; Gladfelter et al., 2006). One example is the mitotic nucleus of Fig. 1B, the SPBs and cMT arrays of which are modeled in Fig. 2B1. All three cMTs emanating at one of the SPBs point backwards. In addition, Fig. 1B shows that one of these cMTs is already aligned at the cortex and, after mitosis, could pull the attached daughter nucleus backwards most likely bypassing one nucleus. The likelihood of a daughter nucleus to emanate cMTs

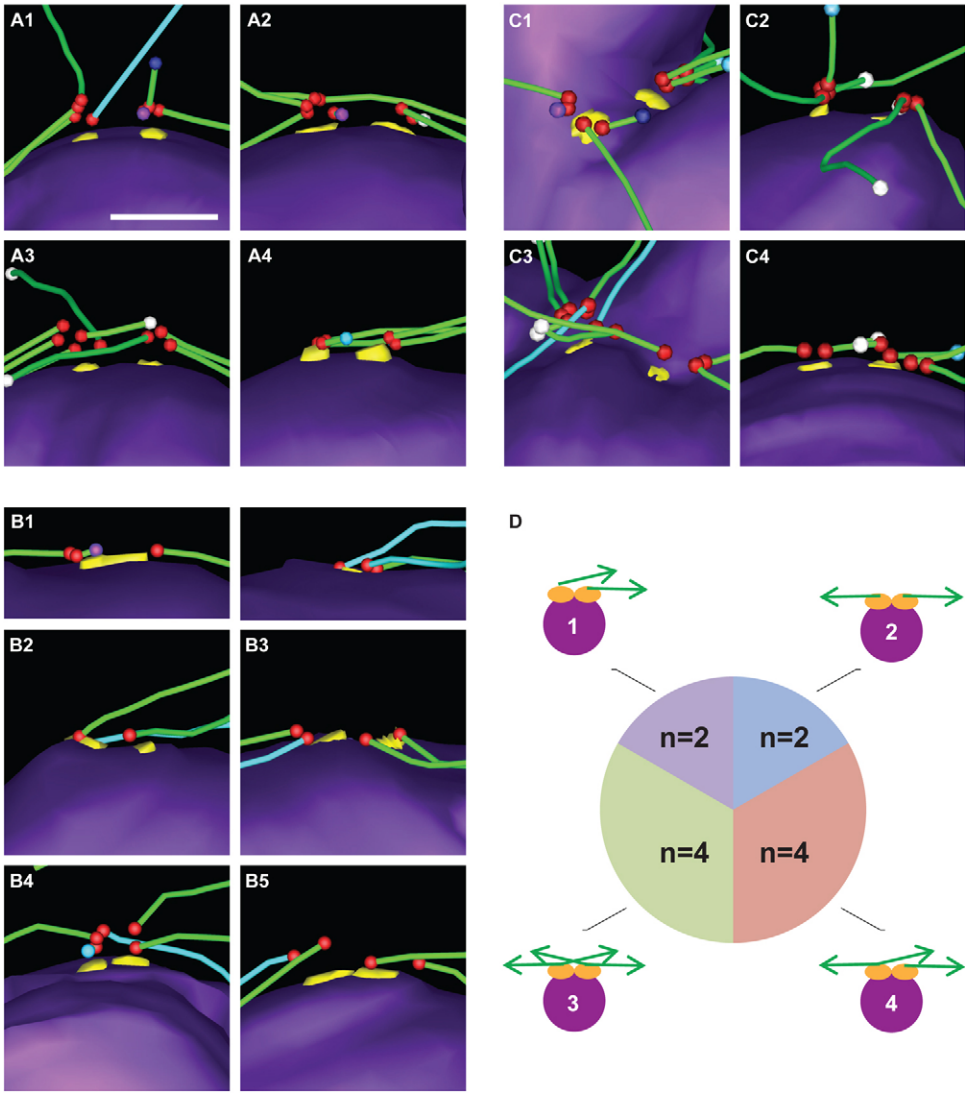

Fig. 2. Directionality of microtubules nucleated at individual SPB. (**A1–C4**) Isolated views of SPBs from nuclei within hyphae A–C classified according to the directionality of nucleated microtubules (nuclear envelope, purple; SPBs, yellow; microtubules, green; microtubule minus-ends, red dots). (**D**) Classification of non-mitotic SPBs ($n=12$) with schematic of the classes: 1, duplicated SPBs with both SPBs emanating cMTs in one same direction (A4,B2); 2, duplicated SPBs with one SPB emanating cMTs in one direction and the other SPB emanating cMTs in the other direction (B3,B5); 3, duplicated SPBs with cMTs emanating from both SPBs in two opposite directions (>90°) (A1,A3,C3,C4); 4, duplicated SPBs with one SPB emanating cMTs in one direction and the other SPB in two opposite directions (A2,B4,C1,C2). Scale bar: 300 nm.

pointing in one direction is high since the average number per SPB is only 3.07±1.27 ($n=28$) very similar to *S. cerevisiae* with 3.14±1.35 cMTs per SPB during nuclear congression ($n=14$; R.G., unpublished observation).

Analysis of cMTs end structure

In previous electron tomography studies based on similar specimen preparation techniques, MT end structure could be correlated with MT polarity (O'Toole et al., 1999; O'Toole et al., 2003; Höög et al., 2007). In *A. gossypii*, we identified five different structures at cMT ends as shown in Fig. 3A–E. These correspond to the five end-morphologies previously described in other organisms. In budding yeast in which SPBs are also the sole site of MT nucleation, it is accepted that capped MT ends associated with SPBs are minus-ends (Fig. 3A). The identified capped ends of cMTs are marked with red dots in the three hyphae (Fig. 3G) and all are associated with the cytoplasmic side of SPBs. Open ends found at the other extremity of cMTs are consequently plus-ends. Depending on the growth state, plus-ends adopt different morphologies. Polymerizing cMTs display sheet-end morphologies (Fig. 3B, yellow dots in Fig. 3G), flared ends (Fig. 3C, light blue dots in Fig. 3G) or meta-stable blunt ends (Fig. 3D, dark blue dots in Fig. 3G), while depolymerizing plus-ends show curling "rams horn"-like structures (Fig. 3E, violet dots in Fig. 3G). Therefore, the classification of MT ends is a basis to determine the ratio of growing and shrinking cMTs in *A. gossypii* hyphae. The frequencies of the clearly identifiable plus-end structures are plotted in Fig. 3F: 80% of MT ends are growing and 20% are shrinking in the three hyphae.

In a recent study *in vivo* polymerization and depolymerization rates of *A. gossypii* cMTs were directly measured and only 6% of the cMTs were found to shrink (Grava and Philippsen, 2010). This apparent discrepancy can be explained by the different methods used. In the *in vivo* study only long and not short cMTs could be monitored because the measured depolymerization rate of 1.5 microns per 6 seconds, the time between two images, is too fast to capture short shrinking cMTs. In contrast, in the 3D reconstructions presented in Figs 2 and 3 the plus-ends of cMTs even shorter than 100 nm could be analyzed in a single snap-shot. This investigation shows that four out of ten curled morphologies were observed on short cMTs (<100 nm) and that those four ends are out of the five identified plus-end of such short cMTs, suggesting that short cMTs shrink more frequently than long cMTs.

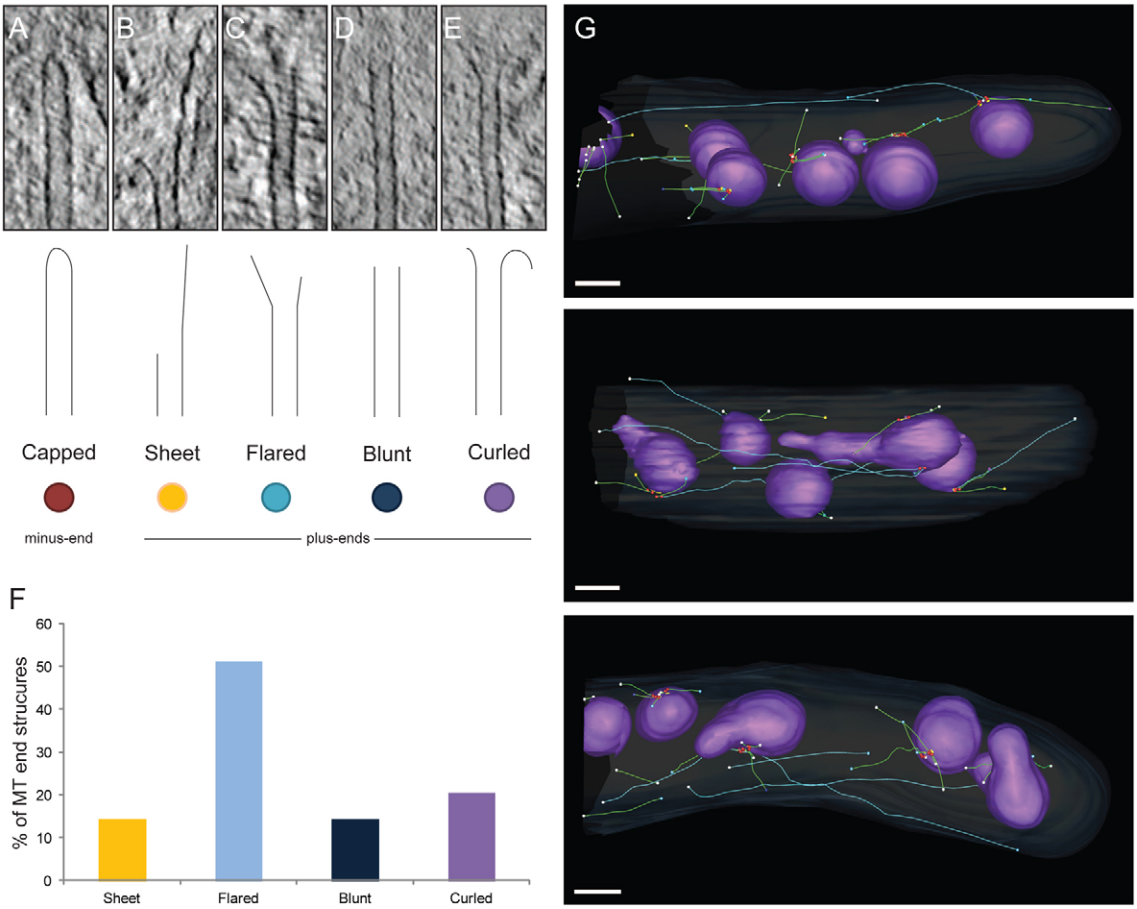

Fig. 3. Distribution of cytoplasmic microtubule end morphologies. (**A–E**) Microtubule end morphologies: (A) capped end, (B) sheet end, (C) flared end, (D) blunt end and (E) curled end, with corresponding cartoons and color codes. (**F**) Distribution of determined cMT plus-ends into morphology classes; the determined plus-ends represent 53% of the total plus-ends. (**G**) Spatial distribution of cMT ends in hyphae A-C; undefined ends are color-coded in white. All MTs are nucleated from an SPB. Scale bars: 1 μm.

Frequencies of nuclei with single and duplicated SPBs

Nuclei in *A. gossypii* are in constant motion and divide asynchronously, which can lead to considerable heterogeneity in terms of nuclear cycle stages in tip regions of different hyphae. Therefore, the very high ratio of nuclei with side-by-side SPBs in the few sampled tip regions modeled in Fig. 1 is most likely not representative for nuclear cycle stages. We therefore performed serial thin section EM to determine the frequency of nuclei with single, duplicated and mitotic SPBs (Fig. 4A–C). We examined a total of 69 nuclei in two independent experiments and found that on average 28.8% contained unduplicated SPBs, 40.8% contained side-by side SPBs and 30.4% contained two SPBs connected by a bipolar spindle (Fig. 4D). This result confirms that a high proportion of *A. gossypii* nuclei carry duplicated side-by-side SPBs. Because SPBs are thought to duplicate at the end of G1 phase (Jaspersen and Winey, 2004; Nair et al., 2010), this data indicates that there is an extended G2 phase during the nuclear cycles of *A. gossypii*. A delay in G2 rather than G1 phase could help to maintain the integrity of genomes since DNA has replicated and a template for repair is available. In addition, having two SPBs also increases the variability of cMT arrays as shown above, which influences cMT-driven nuclear movements, so this variation on nuclear cycle regulation may be advantageous for multinuclearity.

Relationship between predicted and experimentally-determined nuclear bypassing

Quantitative measurements of nuclear bypassing events during different stages of *A. gossypii* nuclear cycles have not been performed yet. Technically this is very demanding because the timing of SPB duplication with S-phase in multinucleated hyphae cannot be monitored with the *in vivo* imaging methods presently available. One clearly identifiable landmark is the separation of nuclei at early anaphase visible in hyphae expressing GFP-tagged histone H4 (Alberti-Segui et al., 2001). Using this landmark nuclear cycle times were found to be heterogeneous (from 46 to 147 minutes) and to last 90 minutes ($n=29$) on average under conditions of time-lapse image acquisitions (Gladfelter et al., 2006; unpublished data). This study also revealed another but less reliable landmark, a frequently observed decrease in nuclear GFP fluorescence intensity in mitosis soon followed by an increase in nuclear fluorescence most likely representing S-phase. The decreased fluorescence of G1 nuclei can help to monitor these nuclei during bypassing.

The results of nuclear pedigree analyses after monitoring mitoses and bypassing in 16 hyphae starting with 108 nuclei are presented in supplementary material Table S1. In 45% (37/80) of mitoses one daughter nucleus bypassed an adjacent nucleus within 15 minutes after the separation of two GFP-labeled

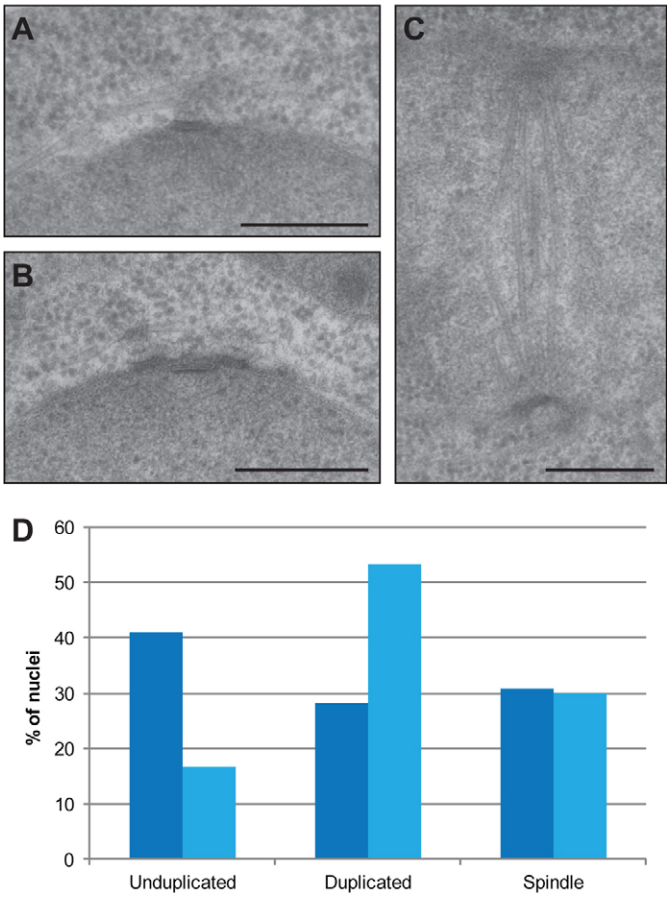

Fig. 4. Frequencies of nuclei containing single and duplicated SPBs. (**A–C**) Representative thin section EM images of the different duplication states of SPB: (A) single SPB, (B) duplicated side-by-side SPBs and (C) mitotic SPBs. The maximal diameters of nuclei with one SPB, two side-by-side SPBs and separated SPBs were determined. No significant differences were found. Scale bars: 300 nm. (**D**) Classification of the SPB states of nuclei from two independent experiments ($n=30$ and 39) using the same strain with GFP-tagged histone H4. The variations between the results of the two experiments might originate from differences in culture conditions (see Materials and Methods) but more probably from the considerable differences in nuclear cycle times (Gladfelter et al., 2006; Nair et al., 2010), which make random sampling difficult.

daughter nuclei (early anaphase). An additional 29 bypassing events were observed after the time window of 15 minutes, the earliest of which was 27 minutes and the latest of which was 88 minutes after separation of two daughter nuclei. These later events most likely involved G2 nuclei. As mentioned above, the average nuclear cycle time is 90 minutes; 37 bypassing events of G1 nuclei occurred during the first 15 minutes and, on average, six bypassing events of G2 nuclei during each of the following five 15-minute time intervals. Thus, the chances of a G2 nucleus to bypass is about one-sixth compared to a G1 nucleus. The limited set of data of cMT arrays emanating from side-by-side SPBs (Fig. 2) predicted that two, out of 12 arrangements, could potentially lead to pulling of G2 nuclei past adjacent nuclei and that one out of two arrangements at single SPBs could lead to pulling of G1 nuclei past adjacent nuclei. In a first approximation the data presented in supplementary material Table S1 are in agreement with these predictions. Further refinements have to take into account the length of cMTs in addition to their arrangements because only very long cMTs interacting with the hyphal cortex can induce long-range pulling. The models of Fig. 1 reveal such long cMTs for less than half of the nuclei.

Nucleation capacity for nMTs of mitotic SPBs

During the serial thin section EM analysis of *A. gossypii* nuclei, we also obtained cross section views of mitotic spindles, which revealed, in the central region of the spindle, an unexpected high number of over 25 nMTs (supplementary material Fig. S1A). This number is comparable to the ~20–24 nMTs that is found at the midzone of the *S. cerevisiae* spindle even though the number of chromosomes in *A. gossypii* is less than half that of budding yeast (Winey et al., 1995; Dietrich et al., 2004). Therefore, it is possible that the capacity of the SPB inner plaque (IP) for the nucleation of microtubules did not adapt during evolution to the changes in chromosome numbers from eight in the common ancestor to seven in *A. gossypii* and 16 in *S. cerevisiae* (Dietrich et al., 2004; Gordon et al., 2009). To further investigate the number of nMTs emanating from the IP structure of *A. gossypii* we used electron tomography and modeled four spindles (Fig. 5A). For comparison, four spindles from *S. cerevisiae* were also modeled (Fig. 5B), and were virtually identical to the established reference (Winey et al., 1995). We found that SPB IP in both organisms serves as a nucleation site for a very similar numbers of nMTs: 22.5 ± 2.78 in *A. gossypii* and 22.38 ± 0.92 in *S. cerevisiae* (Fig. 5C).

The average diameter of an *A. gossypii* SPB based on the width of the CP is 119 ± 21 nm (Lang et al., 2010a), which is very similar to the mitotic CP in haploid *S. cerevisiae* (Byers and Goetsch, 1974; Winey et al., 1995). It is possible that this dimension reflects a minimal size for a functional SPB, which could explain why its size and nMT nucleation capacity remained conserved in *A. gossypii*. It is known that size and microtubule nucleation capacity of SPBs are correlated as they are doubled and quadrupled in diploid and tetraploid *S. cerevisiae* cells, respectively (Byers and Goetsch, 1975; Bullitt et al., 1997). Such correlation cannot be tested in *A. gossypii* because diploid or tetraploid nuclei have not been found yet in this fungus. However, nuclei of an *AgNUD1* gene deletion strain are enlarged most likely due to a ploidy increase (Lang et al., 2010b). The diameter of CPs in this mutant is increased to 174.8 ± 17 nm and these enlarged SPBs can nucleate close to 40 nMTs as concluded from spindle cross sections (supplementary material Fig. S1B), indicating that the ability of the SPB to adjust its size for increased nMT nucleation capacity is conserved in *A. gossypii*.

Conservation of the number of kinetochore and inter-polar MTs

In *S. cerevisiae* the spindle is composed of two distinct populations of MTs nucleated at each SPB: 16 rather short nMTs that attach to kinetochores at each centromere of the 16 chromosomes and depolymerize during anaphase, the kinetochore MTs (kMTs), and around four to six longer ones which interdigitate with microtubules from opposite SPBs to drive spindle elongation, the inter-polar MTs (ipMTs) (Gardner et al., 2008; Winey et al., 1995). These lengths distributions were also found in the four *S. cerevisiae* reference spindles (Fig. 5D). To first assess whether *A. gossypii* nMTs also divide into distinct populations, we looked at the normalized nMT length distribution

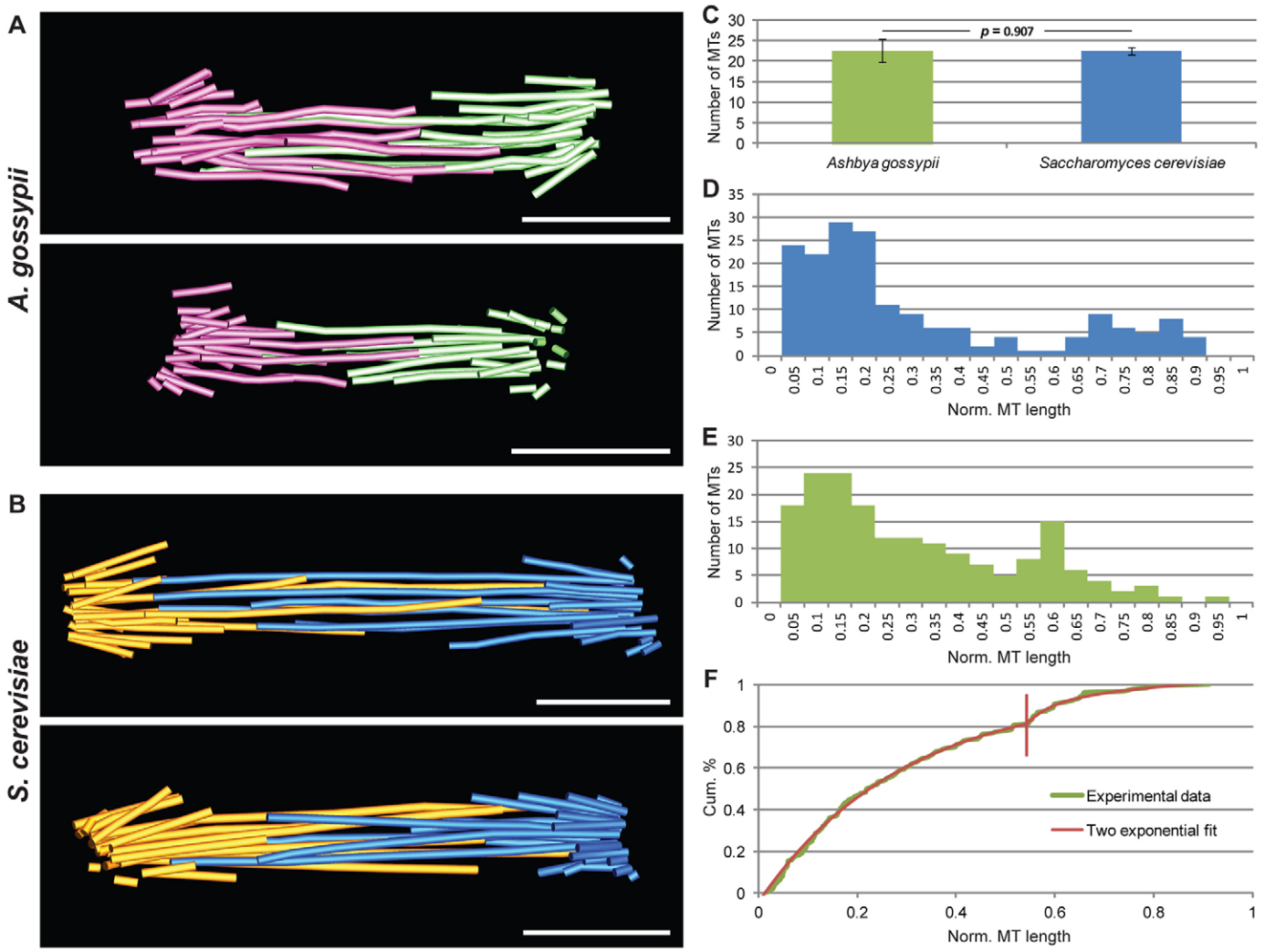

Fig. 5. Organization of bipolar mitotic spindles. (**A**) Model view of *A. gossypii* bipolar mitotic spindles with microtubules from one SPB in green and from the opposite SPB in magenta. (**B**) Model view of *S. cerevisiae* bipolar mitotic spindles with microtubules from one SPB in blue and from the opposite SPB in orange. (**C**) Average number of microtubule nucleated per SPB in *A. gossypii* and *S. cerevisiae* (error bars indicate s.d.). The *P*-value was determined using unpaired unequal variance two-tailed Student's *t*-test. (**D**) Normalized microtubule length distribution in *S. cerevisiae* showing the presence of two distinct microtubule populations. (**E**) Normalized cumulated microtubule length distribution in *A. gossypii* showing the presence of two distinct microtubule populations. (**F**) Normalized cumulated microtubule length distribution in *A. gossypii*. The fitting of two exponential curves delimitates the two populations of short and long microtubules (shown by the red line). The determined threshold (54.31% in length, indicated by vertical red line) distributes the microtubules into proportions of 80.66% and 19.34% of the total number of microtubules. Scale bars: 300 nm.

and could show the existence of two populations, rather short and longer nMTs (Fig. 5E). Because the number of short nMTs is clearly larger than seven, the number of chromosomes in haploid *A. gossypii* nuclei, we analyzed the cumulative normalized MT length distribution and calculated the threshold delimiting the two populations (Fig. 5F). Interestingly, the threshold of 54.31% in length reveals one population represented by 80.66% of short MTs (17.75 MTs) and a second population represented by 19.34% of longer MTs (4.25 MTs). The presence of these two populations implies a regulation like in *S. cerevisiae*: long nMTs regulated by the establishment of antiparallel overlaps corresponding to ipMTs and short nMTs regulated through the connection to kinetochores representing the pool of kMTs. The fact that *A. gossypii* possesses only 7 chromosomes for 17–18 potential kMTs suggests a scheme of multiple MT attachment sites per centromere.

Spatial organization of potential kinetochore MTs

We looked at the spatial distribution of the MT plus-ends of the potential kMTs and ipMTs and compared them to the plus-ends distribution of the kMTs and ipMTs in *S. cerevisiae*. In a perpendicular view of spindles (Fig. 6A), we observed that plus-ends of potential kMTs in *A. gossypii* and of kMTs in *S. cerevisiae* both present a peripheral distribution with respect to the spindle axis (Fig. 6B, left). Moreover, plus-ends of potential ipMTs in *A. gossypii* and of ipMTs in *S. cerevisiae* both preferentially distribute in the center of the spindle (Fig. 6B, right). In *A. gossypii* the population of potential ipMTs locates at

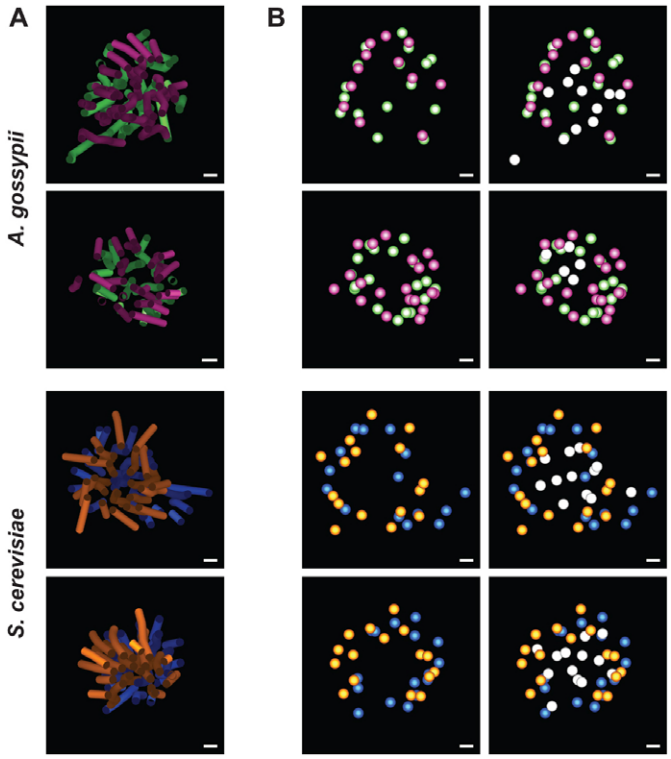

Fig. 6. Organization of potential kinetochore microtubules. (**A**) Perpendicular view of *A. gossypii* and *S. cerevisiae* bipolar mitotic spindle models presented in Fig. 5. (**B**) Perpendicular view of plus-ends of potential kMTs showing their peripheral distribution (color-coded according to the spindle pole they originate from). Right-hand images show plus-ends of potential kMTs together with plus-ends of centrally located ipMTs (white). Scale bars: 30 nm.

an average value of 70.65 ±40.7 nm (s.d.) from the spindle axis with a significant difference (P-value=0.0286; unpaired unequal variance two-tailed Student's t-test) with the distribution of potential kMT population, which locates at an average value of 87.38 ±28.5 nm. In *S. cerevisiae* the ipMTs are located at an average value of 66.1 ±32.9 nm, while kMTs locate at 96.7 ±37.4 nm (P-value, 6.77×10^{-7}; unpaired unequal variance two-tailed Student's t-test). This difference is further evidence that the two populations correspond to the two predicted classes of nMTs and that two or three kMTs are likely binding one centromere.

Discussion

Our aim was to better understand the organization of the MT cytoskeleton and its role in the cMT-dependent and dynein-driven movements of nuclei in multinucleated hyphae of *A. gossypii*. We showed that the majority of the nuclei carry two side-by-side SPBs and that the number, but not the direction, of cMTs is controlled. On average, each SPB nucleates an independent array of three cMTs, one of which is often 3 microns or longer and has a plus-end structure typical for growing MTs. The longer the cMT, the higher the probability that it aligns along the cortex where dynein, transported from the minus ends at SPBs to the plus-ends of cMTs independent of their orientation, associates with cortical proteins and exerts pulling forces for a limited time (Grava et al., 2011). The majority of the double cMT arrays nucleated at side-by-side SPBs emanate long cMTs in opposite directions with respect to the growth axis. This arrangement can explain the frequently observed bidirectional movements of nuclei, pulling for a few microns in one direction followed by pulling in the opposite direction with a net movement adjusted to the growth speed of the hypha. When similar pulling forces are exerted in both directions nuclei tumble showing only short-angle rotational movements, as recently described (Lang et al., 2010a).

In two out of the twelve modeled double cMT arrays, all long cMTs emanate in one direction, which would allow long-range pulling in the direction of the MTs and thus nuclear bypassing if the pulling cMT has grown beyond adjacent nuclei. The modeled hyphae document examples of such very long cMTs. Nuclear pedigree analysis showed that daughter nuclei after mitotic divisions are often involved in long-range bypassing. Because these nuclei contain a single unduplicated SPB, the chance that all cMTs are oriented in one direction is greater than if nuclei had two SPBs and two cMT arrays. These observations explain the observed high frequency of nuclear bypassing for daughter nuclei (Alberti-Segui et al., 2001; Gladfelter et al., 2006). An efficient mechanism for nuclear bypassing is of advantage in multinucleated hyphae because it allows nuclear mixing (Roper et al., 2011). Without nuclear mixing a detrimental mutation for example in the leading nucleus of a hypha, will be inherited to all daughter nuclei in this region thereby impairing future growth. Fungal systems which perform nuclear bypassing should also have a rescue mechanism if bypassing nuclei entangle in the narrow hypha which could lead to the aggregation of nuclei. The bi-directional pulling of nuclei serves as such rescue mechanism in *A. gossypii* because nuclear cluster form in mutants with reduced bi-directional movements (Grava et al., 2011). Thus, the cMT cytoskeleton of *A. gossypii* successfully adapted to the new demands during evolution from mono-nucleated budding yeast-like cells to continuously elongating multinucleated hyphae.

Interestingly, nuclei in *A. gossypii* hyphae spend little time in the G1 state, in which the SPB remains unduplicated. The fact that a substantial fraction of nuclei contain duplicated side-by-side SPBs strongly points to a prolonged period in G2 phase of the nuclear cycle. Pausing at this stage is advantageous for a haploid organism in that chromosomes have been replicated – if one copy of a gene or chromosome is damaged a template for repair by homologous recombination is available, thus limiting chromosome rearrangements and other types of error-based types of DNA damage repair.

Unlike the cMT cytoskeleton, the nMT cytoskeleton appears to have remained largely unaltered during the evolution from a budding yeast-like ancestor. Previous studies had already hinted at this possibility. For instance, mitotic spindles observed by immunofluorescence or live-cell imaging using GFP-tagged tubulin have similar dimensions in both organisms and mitosis proceeds with similar kinetics and without nuclear envelope breakdown (Gladfelter et al., 2006; Alberti-Segui et al., 2001; Lang et al., 2010a; Finlayson et al., 2011). What was unexpected however, is the fact that the number of nMTs appears to also be conserved. Despite the fact that *A. gossypii* nuclei carry only 7 and not 16 chromosomes like *S. cerevisiae*, we did not see significant differences with respect to the nMT nucleation capacity of the SPB or the length and number of presumptive kMTs and ipMTs. The surprisingly similar dimensions of the SPBs in both organisms may reflect the minimal size of a functional SPB, which nucleates 22 nMTs on average. The extra

nMTs are used in *A. gossypii* to reinforce the attachment of each chromosome to the spindle by one additional kMT while in *S. cerevisiae* the limited capacity of the IP to nucleate nMT also limited the attachment of each of the 16 chromosomes to a single kMT.

An interesting question is how *S. cerevisiae* uses one kMT per chromosome and how *A. gossypii* might use two. *A. gossypii* chromosomes have ~180 bp point centromeres (Dietrich et al., 2004) rather than the ~125 bp centromere of *S. cerevisiae* (Cottarel et al., 1989), and therefore may form two centromeric nucleosomes (Meraldi et al., 2006) to accommodate more than one kMT. Higher numbers of ipMTs and kMTs could both be necessary for accurate chromosome segregation in a multinucleated organism. Indeed, due to the fact that nuclei within the *A. gossypii* mycelium are highly dynamic also during nuclear division (Alberti-Segui et al., 2001), the spindle must withstand additional forces not observed in the unicellular organisms like budding yeast.

Materials and Methods

Sample preparation for thin section TEM

The thin section SPB duplication analysis was performed in two independent and different manners. In the first analysis, *AgH4GFP* spores (Helfer and Gladfelter, 2006) were grown for 12 hours at 30℃ in AFM (10 g/l yeast extract, 10 g/l peptone, 20 g/l glucose, 0.3 g/l Myo-Inositol). The cells were frozen on a Leica EM-Pact at ~2050 bar, then transferred under liquid nitrogen into 2% osmium tetroxide/0.1% uranyl acetate/acetone and transferred to the Leica AFS. The freeze substitution protocol was as follows: −90℃ for 16 hours, up 4℃/hour for 7 hours, −60℃ for 19 hours, up 4℃/hour for 10 hours, −20℃ for 20 hours. Samples were then removed from the AFS and placed in the refrigerator for 4 hours, then allowed to incubate at room temperature for 1 hour. Samples went through three changes of acetone over 1 hour and were removed from the planchettes. Then, they were embedded in acetone/Epon mixtures to final 100% Epon over several days in a stepwise procedure as described (McDonald, 1999). Serial thin sections of 60 nm were cut on a Leica UC6, stained with uranyl acetate and Sato's lead and imaged on a FEI Tecnai Spirit (Hillsboro, OR). Serial section images were aligned using AutoAligner (Bitplane AG, Zurich, Switzerland).

For the second analysis, samples were processed as described previously (Höög and Antony, 2007) with some modifications. *A. gossypii AgH4GFP* spores (Helfer and Gladfelter, 2006) were grown in liquid YPD (10 g/l yeast extract, 20 g/l peptone, 20 g/l glucose) supplemented with 1 g/l Myo-inositol and tetracycline for 10 hours at 30℃. Cells were collected onto a polycarbonate filter (Milipore) and cryoimmobilized by high-pressure freezing using Leica EMPACT-2 (Leica Microsystems, Vienna, Austria). Freeze substitution of the cells was done using a freeze substitution device EM-AFS2 (Leica Microsystems, Vienna, Austria). The freeze substitution solution contained 0.2% uranyl acetate, 0.1% glutaraldehyde and 1% water dissolved in anhydrous acetone, and the samples were substituted at −90℃ for 50 hours. The temperature was then increased at a rate of 5℃/hour to −45℃ followed by 5 hours incubation at −45℃. The samples were rinsed with acetone three times for 10 minutes, followed by lowicryl HM20 (Polysciences, Warrington, PA) infiltration at −45℃ with 25% lowicryl in acetone for 2 hours, 50% lowicryl for 2 hours and 75% lowicryl for 2 hours. The samples were then left in 100% lowicryl for 12 hours and in new 100% lowicryl for 2 hours before onset of polymerization. UV polymerization was applied for 48 hours at −45℃ and then the temperature was increased to 20℃ at a rate of 5℃/hour and the samples were left exposed to UV at room temperature for 48 hours. Thin sections (60–70 nm) were cut using a Reichert Ultracut-E microtome (Leica Microsystems, Vienna, Austria) and collected on Formvar-coated palladium-copper slot grids. Sections were post-stained with 4% uranyl acetate in 70% methanol for 2 minutes, and then with lead citrate for 30 seconds. Image were acquired on a Biotwin CM120 TEM (FEI, Eindhoven, NL).

Electron tomography

Serial thick sections of lowicryl embedded samples (300 nm thick) were cut using a Reichert Ultracut-E microtome (Leica Microsystems, Vienna, Austria) and collected on Formvar-coated palladium-copper slot grids. Sections were post-stained with 4% uranyl acetate in 70% methanol for 10 minutes, then with lead citrate for 3 minutes. Digital images were taken at 300 kV from −60° to +60° tilt with 1° increment on a Tecnai F30 electron microscope equipped with an Eagle 4K CCD camera (FEI, Eindhoven, NL). Montaged tomograms of 1×3 frames were used to acquire hyphae of around 11 µm long at a magnification of 12,000×. The tilted images were aligned and montaged tomograms collected from adjacent serial sections were generated by R-weighted back projection, joined in z, modeled and analyzed using the IMOD software (Kremer et al., 1996).

Acknowledgements

We thank the members of the Antony group and the EMBL Electron Microscopy Core Facility for helpful discussions and technical support. We thank especially Charlotta Funaya and Sabine Pruggnaller for their crucial involvement in sample preparation, tomograms acquisition and modeling. We are also grateful to François Nédélec and his group for support and discussions. We thank Sandrine Grava for providing *A. gossypii* spores and protocols.

Funding

This work is supported by a postdoctoral grant from BIOMS (Center for Modelling and Simulation in the Biosciences) to A.Z.P.; and the Stowers Institute for Medical Research and the American Cancer Society [grant number RSG-11-030-01-CSM to S.L.J.]. Part of the work was supported by the Swiss National Science Foundation [grant number 3100A0-112688 to P.P.].

Supplementary material available online at
http://jcs.biologists.org/lookup/suppl/doi:10.1242/jcs.111005/-/DC1

References

Alberti-Segui, C., Dietrich, F. S., Altmann-Jöhl, R., Hoepfner, D. and Philippsen, P. (2001). Cytoplasmic dynein is required to oppose the force that moves nuclei towards the hyphal tip in the filamentous ascomycete *Ashbya gossypii*. *J. Cell Sci.* **114**, 975-986.

Bullitt, E., Rout, M. P., Kilmartin, J. V. and Akey, C. W. (1997). The yeast spindle pole body is assembled around a central crystal of Spc42p. *Cell* **89**, 1077-1086.

Byers, B. and Goetsch, L. (1974). Duplication of spindle plaques and integration of the yeast cell cycle. *Cold Spring Harb. Symp. Quant. Biol.* **38**, 123-131.

Byers, B. and Goetsch, L. (1975). Electron microscopic observations on the meiotic karyotype of diploid and tetraploid Saccharomyces cerevisiae. *Proc. Natl. Acad. Sci. USA* **72**, 5056-5060.

Cottarel, G., Shero, J. H., Hieter, P. and Hegemann, J. H. (1989). A 125-base-pair CEN6 DNA fragment is sufficient for complete meiotic and mitotic centromere functions in Saccharomyces cerevisiae. *Mol. Cell. Biol.* **9**, 3342-3349.

Dietrich, F. S., Voegeli, S., Brachat, S., Lerch, A., Gates, K., Steiner, S., Mohr, C., Pöhlmann, R., Luedi, P., Choi, S. et al. (2004). The *Ashbya gossypii* genome as a tool for mapping the ancient *Saccharomyces cerevisiae* genome. *Science* **304**, 304-307.

Finlayson, M. R., Helfer-Hungerbühler, A. K. and Philippsen, P. (2011). Regulation of exit from mitosis in multinucleate *Ashbya gossypii* cells relies on a minimal network of genes. *Mol. Biol. Cell* **22**, 3081-3093.

Gardner, M. K., Haase, J., Mythreye, K., Molk, J. N., Anderson, M., Joglekar, A. P., O'Toole, E. T., Winey, M., Salmon, E. D., Odde, D. J. et al. (2008). The microtubule-based motor Kar3 and plus end-binding protein Bim1 provide structural support for the anaphase spindle. *J. Cell Biol.* **180**, 91-100.

Gladfelter, A. S., Hungerbuehler, A. K. and Philippsen, P. (2006). Asynchronous nuclear division cycles in multinucleated cells. *J. Cell Biol.* **172**, 347-362.

Gordon, J. L., Byrne, K. P. and Wolfe, K. H. (2009). Additions, losses, and rearrangements on the evolutionary route from a reconstructed ancestor to the modern *Saccharomyces cerevisiae* genome. *PLoS Genet.* **5**, e1000485.

Grava, S. and Philippsen, P. (2010). Dynamics of multiple nuclei in *Ashbya gossypii* hyphae depend on the control of cytoplasmic microtubules length by Bik1, Kip2, Kip3, and not on a capture/shrinkage mechanism. *Mol. Biol. Cell* **21**, 3680-3692.

Grava, S., Keller, M., Voegeli, S., Seger, S., Lang, C. and Philippsen, P. (2011). Clustering of nuclei in multinucleated hyphae is prevented by dynein-driven bidirectional nuclear movements and microtubule growth control in *Ashbya gossypii*. *Eukaryot. Cell* **10**, 902-915.

Han, G., Liu, B., Zhang, J., Zuo, W., Morris, N. R. and Xiang, X. (2001). The *Aspergillus* cytoplasmic dynein heavy chain and NUDF localize to microtubule ends and affect microtubule dynamics. *Curr. Biol.* **11**, 719-724.

Helfer, H. and Gladfelter, A. S. (2006). AgSwe1p regulates mitosis in response to morphogenesis and nutrients in multinucleated *Ashbya gossypii* cells. *Mol. Biol. Cell* **17**, 4494-4512.

Höög, J. L. and Antony, C. (2007). Whole-cell investigation of microtubule cytoskeleton architecture by electron tomography. *Methods Cell Biol.* **79**, 145-167.

Höög, J. L., Schwartz, C., Noon, A. T., O'Toole, E. T., Mastronarde, D. N., McIntosh, J. R. and Antony, C. (2007). Organization of interphase microtubules in fission yeast analyzed by electron tomography. *Dev. Cell* **12**, 349-361.

Jaspersen, S. L. and Winey, M. (2004). The budding yeast spindle pole body: structure, duplication, and function. *Annu. Rev. Cell Dev. Biol.* **20**, 1-28.

Köhli, M., Galati, V., Boudier, K., Roberson, R. W. and Philippsen, P. (2008). Growth-speed-correlated localization of exocyst and polarisome components in growth zones of *Ashbya gossypii* hyphal tips. *J. Cell Sci.* **121**, 3878-3889.

Kremer, J. R., Mastronarde, D. N. and McIntosh, J. R. (1996). Computer visualization of three-dimensional image data using IMOD. *J. Struct. Biol.* **116**, 71-76.

Lang, C., Grava, S., van den Hoorn, T., Trimble, R., Philippsen, P. and Jaspersen, S. L. (2010a). Mobility, microtubule nucleation and structure of microtubule-organizing centers in multinucleated hyphae of *Ashbya gossypii*. *Mol. Biol. Cell* **21**, 18-28.

Lang, C., Grava, S., Finlayson, M., Trimble, R., Philippsen, P. and Jaspersen, S. L. (2010b). Structural mutants of the spindle pole body cause distinct alteration of cytoplasmic microtubules and nuclear dynamics in multinucleated hyphae. *Mol. Biol. Cell* **21**, 753-766.

Lew, D. J. and Reed, S. I. (1993). Morphogenesis in the yeast cell cycle: regulation by Cdc28 and cyclins. *J. Cell Biol.* **120**, 1305-1320.

McDonald, K. (1999). High-pressure freezing for preservation of high resolution fine structure and antigenicity for immunolabeling. *Methods Mol. Biol.* **117**, 77-97.

Meraldi, P., McAinsh, A. D., Rheinbay, E. and Sorger, P. K. (2006). Phylogenetic and structural analysis of centromeric DNA and kinetochore proteins. *Genome Biol.* **7**, R23.

Minke, P. F., Lee, I. H., Tinsley, J. H., Bruno, K. S. and Plamann, M. (1999). *Neurospora crassa ro-10* and *ro-11* genes encode novel proteins required for nuclear distribution. *Mol. Microbiol.* **32**, 1065-1076.

Morris, N. R. (2000). Nuclear migration. From fungi to the mammalian brain. *J. Cell Biol.* **148**, 1097-1102.

Nair, D. R., D'Ausilio, C. A., Occhipinti, P., Borsuk, M. E. and Gladfelter, A. S. (2010). A conserved G1 regulatory circuit promotes asynchronous behavior of nuclei sharing a common cytoplasm. *Cell Cycle* **9**, 3771-3779.

O'Toole, E. T., Winey, M. and McIntosh, J. R. (1999). High-voltage electron tomography of spindle pole bodies and early mitotic spindles in the yeast *Saccharomyces cerevisiae*. *Mol. Biol. Cell* **10**, 2017-2031.

O'Toole, E. T., McDonald, K. L., Mäntler, J., McIntosh, J. R., Hyman, A. A. and Müller-Reichert, T. (2003). Morphologically distinct microtubule ends in the mitotic centrosome of *Caenorhabditis elegans*. *J. Cell Biol.* **163**, 451-456.

Roper, M., Ellison, C., Taylor, J. W. and Glass, N. L. (2011). Nuclear and genome dynamics in multinucleate ascomycete fungi. *Curr. Biol.* **21**, R786-R793.

Schuster, M., Lipowsky, R., Assmann, M. A., Lenz, P. and Steinberg, G. (2011). Transient binding of dynein controls bidirectional long-range motility of early endosomes. *Proc. Natl. Acad. Sci. USA* **108**, 3618-3623.

Seiler, S., Plamann, M. and Schliwa, M. (1999). Kinesin and dynein mutants provide novel insights into the roles of vesicle traffic during cell morphogenesis in *Neurospora*. *Curr. Biol.* **9**, 779-785.

Wedlich-Söldner, R., Schulz, I., Straube, A. and Steinberg, G. (2002). Dynein supports motility of endoplasmic reticulum in the fungus *Ustilago maydis*. *Mol. Biol. Cell* **13**, 965-977.

Winey, M., Mamay, C. L., O'Toole, E. T., Mastronarde, D. N., Giddings, T. H., Jr, McDonald, K. L. and McIntosh, J. R. (1995). Three-dimensional ultrastructural analysis of the Saccharomyces cerevisiae mitotic spindle. *J. Cell Biol.* **129**, 1601-1615.

Xiang, X. and Fischer, R. (2004). Nuclear migration and positioning in filamentous fungi. *Fungal Genet. Biol.* **41**, 411-419.

Xiang, X., Beckwith, S. M. and Morris, N. R. (1994). Cytoplasmic dynein is involved in nuclear migration in Aspergillus nidulans. *Proc. Natl. Acad. Sci. USA* **91**, 2100-2104.

Zekert, N. and Fischer, R. (2009). The *Aspergillus nidulans* kinesin-3 UncA motor moves vesicles along a subpopulation of microtubules. *Mol. Biol. Cell* **20**, 673-684.

Zhang, J., Li, S., Fischer, R. and Xiang, X. (2003). Accumulation of cytoplasmic dynein and dynactin at microtubule plus ends in *Aspergillus nidulans* is kinesin dependent. *Mol. Biol. Cell* **14**, 1479-1488.